

CONCISE ARTICLE

[View Article Online](#)
[View Journal](#) | [View Issue](#)

Developing novel C-4 analogues of pyrrole-based antitubulin agents: weak but critical hydrogen bonding in the colchicine site†

Cite this: *Med. Chem. Commun.*, 2013, **4**, 417Chenxiao Da,^a Nakul Telang,^b Kayleigh Hall,^b Emily Kluball,^b Peter Barelli,^b Kara Finzel,^b Xin Jia,^b John T. Gupton,^b Susan L. Mooberry^c and Glen E. Kellogg^{*a}Received 24th October 2012
Accepted 10th December 2012

DOI: 10.1039/c2md20320k

www.rsc.org/medchemcomm

The synthesis, biological evaluation and molecular modeling of a series of pyrrole compounds related to 3,5-dibromo-4-(3,4-dimethoxyphenyl)-1H-pyrrole-2-carboxylic acid that evaluates and optimizes C-4 substituents are reported. The key factor for microtubule depolymerization activity appears to be the presence of an appropriately positioned acceptor for Cys241β in the otherwise hydrophobic subpocket A.

Introduction

Microtubules have been recognized as a target for cancer treatment for a long period of time, owing to their multifarious and critical functions in eukaryotic cells, such as maintenance of cell shape, protein trafficking, signaling and segregation of chromosomes during mitosis. Traditionally, microtubule-targeting agents are classified as microtubule stabilizing or destabilizing agents based on their effects on microtubule polymer mass at high concentrations. A more practical classification in terms of drug design divides them according to their binding sites on tubulin, which are the taxane domain, the vinca domain, the colchicine site and new sites discovered as more structurally diverse agents are developed.¹ Unlike the taxanes and vinca alkaloids, neither colchicine (**1**) nor any colchicine site agents have been successful in cancer chemotherapy due to their severe toxicity to normal tissues.² However, as an alternative to conventional therapy, the combretastatins, which also bind in the colchicine site, have been extensively developed and some are progressing through clinical trials (including Phase III) as antitumor vascular disrupting agents.^{1,3} Moreover, a recent study highlighted that colchicine site agents might be able to circumvent βIII-tubulin overexpression, which is related to the emerging drug resistance to taxanes and vinca alkaloids.⁴

We previously reported the synthesis and modeling of a series of pyrrole-based antitubulin agents targeting the colchicine site⁵ and predicted, based on a series of C-2 analogues, two distinct binding modalities distinguishing highly active analogues from those with weaker activities.⁶ The most active analogue, 3,5-dibromo-4-(3,4-dimethoxyphenyl)-1H-pyrrole-2-carboxylic acid ethyl ester (**2**, JG-03-14, Fig. 1), demonstrated potent antiproliferative activity against a wide range of cancer cell lines, strong microtubule-destabilizing activity and is a poor substrate of the P-glycoprotein drug efflux pump that transports taxanes and vinca alkaloids.⁷ Further studies showed that the compound disrupts multiple endothelial cell functions, suggesting the potential for vascular-disrupting activities.⁸ In this respect, **2** has become a valuable lead candidate and the five atoms on its pyrrole scaffold can be easily modified for structural-activity relationships (SAR), providing a basis for the future optimization and development.

In this study, we retained the two bromine groups at C-3 and C-5 and the ethyl ester at the C-2 position and focused on modifications to the 3,4-dimethoxyphenyl ring at the C-4 position. Previously, we showed that **2**'s ethyl ester at C-2 is an ideally suited substituent for that position and this induces the 3,4-dimethoxyphenyl moiety of **2** to overlap with ring A of colchicine in the colchicine site and bind in a subpocket formed mainly by hydrophobic residues and one polar residue, Cysβ241.⁶ Here, we

^aDepartment of Medicinal Chemistry & Institute for Structural Biology and Drug Discovery, Virginia Commonwealth University, Richmond, Virginia, USA 23298-0540. E-mail: glen.kellogg@vcu.edu; Tel: +1 804 828-6452

^bDepartment of Chemistry, Gottwald Center for the Sciences, University of Richmond, Richmond, Virginia, USA 23173

^cDepartment of Pharmacology, University of Texas Health Science Center at San Antonio, San Antonio, Texas, USA 78229-3900

† Electronic supplementary information (ESI) available: Experimental details for the synthesis and characterization of reported compounds, procedures for the assays and additional information on the computational methods utilized. See DOI: 10.1039/c2md20320k

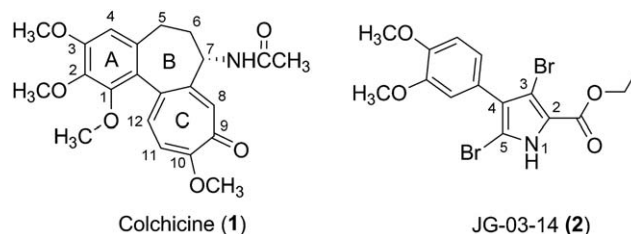


Fig. 1 Structures of colchicine and lead compound JG-03-14.

explore the electronic, hydrogen bonding and hydrophobic characteristics of substituents at C-4 to enrich our understanding of the SAR of these compounds. We report here the integrated synthesis, microtubule depolymerizing and antiproliferative effects and modeling results for a focused set of analogues.

Results and discussion

Chemistry

We have previously reported⁹ the synthesis of **2** and have utilized a similar strategy (Method A) to prepare analogues **5a–5i** (Table 1); the appropriate aryl vinamidinium salt (**3a–3i**) was condensed with glycine ethyl ester to yield the pyrrole ethyl esters **4a–4i**. For analogues **5j–5p** (Table 1), the ester intermediates **4j–4p** were prepared (Method B) by a Suzuki cross-coupling of 4-bromo-1*H*-pyrrole-2-carboxylic acid ethyl ester (**6**) with the appropriate aryl boronic acid. The final dibromination step for all analogues was accomplished with pyridinium tribromide in DMF. Compound **5q** was prepared by bromination of **2** with dibromodimethylhydantoin. See Scheme S1 (ESI[†]) for synthetic details.

Biological activity

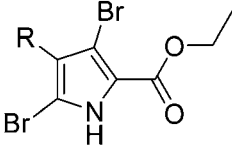
Antiproliferative activities were measured in MDA-MB-435 cancer cells using the sulforhodamine B assay and effects on cellular microtubules were evaluated in A-10 cells using immunofluorescence as previously described.⁷ Results are presented in Table 1.

Structure–activity relationships

All structural modifications for this study were at the C-4 position of the pyrrole core. Antiproliferative activities as well as microtubule depolymerizing activities were measured (Table 1). Compounds **5a–5d** showed very weak or barely any effect on microtubule polymerization with EC₅₀ values greater than 75 μM. Compound **5a**, the unsubstituted ring analogue, showed negligible antiproliferative activity, while this activity for **5b–5d** (especially **5c** with an IC₅₀ of 0.919 μM) likely indicates a different mechanism of action, although some form of microtubule inhibition may still be responsible. For the rest of the compounds, **2** and **5e–5q** (and **1**), the microtubule inhibitory activity correlates well with the antiproliferative activity ($pEC_{50} = 1.10 pIC_{50} - 1.57$, $r^2 = 0.79$, Fig. 2). Interestingly, for these compounds, $pEC_{50} - pIC_{50} = 1.00 \pm 0.43$ μM, which indicates that microtubule inhibition is consistently one order of magnitude weaker than overall inhibition of proliferation.

The SAR was analyzed with respect to the EC₅₀. The active lead compound **2** (0.490 μM) bore two methoxy groups on the phenyl ring attached at the C-4 position. Removing either of the methoxys showed a significant decrease in activity by 14-fold (**5e**, 7.0 μM) and 5-fold (**5f**, 2.4 μM), respectively; as noted above, a complete loss of microtubule inhibitory activity was observed when all ring substitutions were eliminated (**5a**), suggesting the significance of *both* methoxys with a particular preference for the *meta*-methoxy group. When compared to **5e**, replacing the hydrophobic methyl with a more polar trifluoromethyl while

Table 1 Structures, antiproliferative and microtubule inhibitory activities of pyrrole compounds



Cmpd	R	Antiproliferation IC ₅₀ (μM)	Microtubule depolymerization EC ₅₀ (μM)	pEC ₅₀	HINT score
1 (Colchicine)	—	0.016 ± 0.002	0.030	7.52	549
2 (JG-03-14)	3,4-Dimethoxyphenyl	0.036 ± 0.002	0.490	6.31	643
5a	Phenyl	10.3 ± 1.3	>75	3.82 ^b	170
5b	4-Methylphenyl	2.24 ± 0.2	>75	3.82 ^b	579
5c	4-Chlorophenyl	0.919 ± 0.020	>75	3.82 ^b	754
5d	4-Bromophenyl	0.312 ± 0.020	~94 ^a	4.03	815
5e	4-Methoxyphenyl	0.843 ± 0.090	7.0	5.15	563
5f	3-Methoxyphenyl	0.633 ± 0.01	2.4	5.62	558
5g	3,4,5-Trimethoxyphenyl	12.9 ± 1.9	>75	3.82 ^b	124
5h	1-Napthyl	3.24 ± 0.20	7.0	5.15	805
5i	3-Indolyl	1.98 ± 0.20	17.8	4.75	271
5j	4-Trifluoromethoxyphenyl	1.70 ± 0.10	27.1	4.57	649
5k	4-Thiomethylphenyl	0.626 ± 0.020	18.5	4.73	541
5l	3,4-Dichlorophenyl	0.806 ± 0.060	9.9	5.00	1012
5m	3-Fluoro-4-methoxyphenyl	0.539 ± 0.040	14.1	4.85	567
5n	6-Ethoxyl-2-napthyl	1.99 ± 0.20	>75	3.82 ^b	577
5o	1,3-Benzodioxol-6-yl	1.80 ± 0.20	29.7	4.53	428
5p	1,4-Benzodioxan-6-yl	4.36 ± 0.3	20.9	4.68	590
5q	2-Bromo-4,5-dimethoxyphenyl	2.64 ± 0.30	14.0	4.85	781

^a 40% microtubule loss at 75 μM, EC₅₀ ~ 75/(2 × 0.4) = 94 μM. ^b Assumed EC₅₀ = 150 μM.

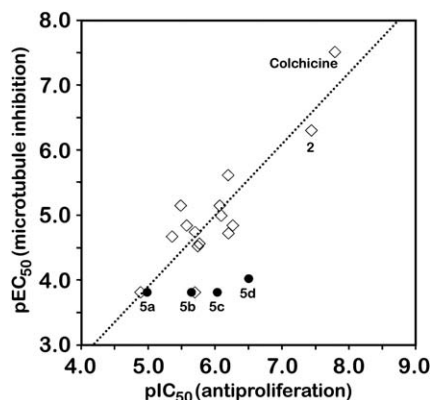


Fig. 2 Correlation of pEC_{50} and pIC_{50} . Compounds indicated by closed circles are not included in correlation. They have high antiproliferative activity but negligible microtubule inhibition, which indicates an alternative mechanism of action.

retaining the acceptor ether oxygen (**5j**) or with the weaker sulfur acceptor (**5k**) resulted in minor losses in activity by 4-fold and 2.5-fold, respectively. Furthermore, attempting to recover activity with hydrophobic groups at the *para*-position with **5b** (methyl), **5c** (chloro) and **5d** (bromo) was completely ineffective with respect to microtubule inhibition, although the antiproliferative activity for these analogues increases with substituent hydrophobicity. Overall, these results suggest that the hydrogen bonding properties of the C-4 ring substituents play the more critical role in microtubule inhibition, although clearly the ether oxygen in $-OMe$ may also serve to place the hydrophobic methyl in a more ideal position.

Addition of a second chlorine at the *meta*-position recovered activity (**5l**, 9.9 μM). This may be partially explained by the weak hydrogen bond accepting character of chlorine, but also its placement in the *meta*-position is a factor – as was seen in the comparison between **5f** and **5e**. Probably because fluorine is less hydrophobic and smaller than chlorine (although a stronger acceptor), the fluorinated compounds, **5m**, was no more effective as a microtubule inhibitor than its des-fluoro analogue **5e**.

The inhibitory activity observed for large aromatic rings as C-4 substituents (**5h** and **5i**) can be attributed to their hydrophobicities and also the hydrogen bond acceptor character of the aromatic π -clouds in naphthyl and indolyl. To further investigate this putative hydrogen bonding, the H-bond acceptor was repositioned with 6-ethoxyl-2-naphthyl at C-4 (**5n**) with negative effect.

Restriction of the rotation of two methyl groups was achieved by first forming a methylene bridge between two oxygens (**5o**), which led to a 60-fold decrease in activity compared to **2**. Secondly, an ethylene bridge (**5p**) fared somewhat better with only a 40-fold activity decrease. Interestingly, addition of a third methoxy to the phenyl ring at its 5-position, as in **5g**, did not lead to the expected increase, but, instead, a total loss in activity; however, placing a bromine at the ring's 2-position and removing the 3-methoxy (**5q**) produced a >5-fold activity increase over **5g**.

Molecular modelling

Modelling was performed to rationalize the observed SAR. The colchicine site is located at the interface of α - and β -tubulin and

mostly buried in β -tubulin. It is surrounded by helices H7 and H8, loop T7 and strands S8 and S9 of β -tubulin and loop T5 of α -tubulin. Comparison of crystal structures of $\alpha\beta$ -tubulin heterodimers complexed with different ligands reveals the flexibility of the colchicine site, especially for loops T7 and T5. To understand the movement of the sidechains and backbones surrounding the site, we performed docking studies with five crystal structures (PDBIDs: 1sa0, 1sa1, 3hkc, 3hkd and 3hke).^{10,11} Docking poses were generated by GOLD¹² and the resulting complexes were minimized in Sybyl with the Tripos forcefield¹³ and rescored with HINT.^{14,15} These results showed that the compounds tended to bind most favorably to the 3hkc model as indicated by higher HINT scores. While 1sa0 is complexed with colchicine and is thus frequently used for docking colchicine site agents, 3hkc, is co-crystallized with the structurally unrelated *N*-{2-[(4-hydroxyphenyl)amino]pyridin-3-yl}-4-methoxybenzenesulfonamide (ESI, Fig. S5†). In docking compounds **2** and **5a–5q**, however, the T5 loop of 3hkc appears to adapt and benefit from hydrogen bonding between the backbone carbonyl of Thr179 α and the pyrrole nitrogen, while in colchicine binding, T5 yields to colchicine's amide chain as seen in 1sa0 (Fig. 3). This binding mode is the same as we previously reported.⁶ The ester chain of **2** and **5a–5q** partially overlaps with ring C of colchicine, fitting into subpocket C with the carbonyl oxygen forming a hydrogen bond with the backbone nitrogen of Val181 α . The pyrrole core locates in the center of the site, forming hydrogen bonds with Asn258 β and Thr179 α . The phenyl moiety overlaps with ring A of colchicine, inserting into the hydrophobic subpocket A, which is formed by Tyr202 β , Val238 β , Thr239 β , Leu242 β , Leu248 β , Leu252 β , Ile378 β and Val318 β , with Leu248 β and Leu255 β clamping the phenyl moiety. One polar residue, Cys241 β , donates to the ligand in the presence of an appropriately positioned acceptor. The presence of this latter residue in subpocket A explains the importance of hydrogen bond accepting character in C-4 substituents observed in the SAR studies.

Detailed analysis of the binding conformations assists further interpretation of the SAR (Fig. 4). In the case of **2**, the thiol hydrogen of Cys241 β is pointed towards the methoxy at the *meta*-position and away from the *para*-position. This was observed for all other cases owing to the steric clashes that the thiol hydrogen could encounter if oriented in the other

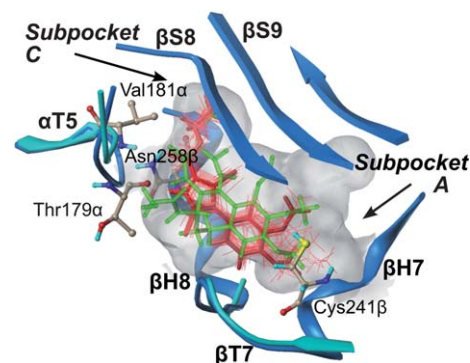


Fig. 3 Colchicine (green) and binding modes of pyrrole-based C-4 analogs in red (compound **2** in heavy sticks). The extents of the colchicine site, as illustrated by MOLCAD, are shown in grayish white.

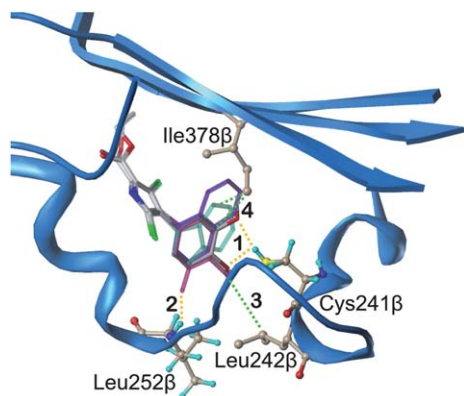


Fig. 4 Specific hydrogen bonding (yellow) and hydrophobic (green) interactions in subpocket A. Compounds **2** (solid white), **5h** (translucent purple), **5i** (translucent green) and **5m** (translucent red) are shown. Notes: (1) the key H-bond interaction is with Cys241 β , which is strongest with the O of methoxy in the ring's *meta* position; (2) some analogues, e.g., with F, can weakly H-bond with the NH of Leu252 β ; (3) the CH₃ of *p*-methoxy has key hydrophobic interactions with Leu242 β ; (4) Ile378 β has hydrophobic interactions with *m*-methoxy or the rings of **5h** or **5i**.

direction. The better hydrogen bonding for a *meta*-position substituent explains the activity of **5f** compared to **5e** and other similar cases. As for **5h** and **5i**, the distal (from the pyrrole core) rings were located directly beneath the thiol hydrogen, thus acting as acceptors for the weak but critical hydrogen bond, but pocket steric issues cancelled this advantage. The fluorine atom of **5m** is also located at the *meta*-position, but the docking study suggested that an 180° ring flip shifted its position in space such that, although the fluorine was anchored by the backbone NH of Leu252 β , it provided no additional bonding to Cys241 β compared to **5e**. In the case of **5g**, the detrimental effect of the third methoxy is visually apparent: the tight distance (3.58 Å) between the backbone of Leu252 β and the phenyl ring of the ligand can lead to significant steric clashes with a large substituent such as the 5-methoxy.

The total HINT scores of C-4 analogues fail to show a tight relationship with pEC₅₀ (ESI, Fig. S6†). However, isolating the HINT score for hydrogen bonding interactions involving Cys241 β for a subset of analogues (**2**, **5e**, **5f**, **5j**, **5k**, **5m** and **5q**) that place, as separate entities, appropriately positioned hydrophobic groups *and* a hydrogen bond acceptor in the subpocket (while not inducing steric clashes),[†] reveals a linear relation with respect to these compounds' pEC₅₀s (Fig. 5). The implications are

[†] Compounds **5a** and **5b** do not possess H-bond acceptor substituents to the phenyl ring. The halogens of **5c**, **5d** and **5l** are considered as weak acceptors by HINT and, while their dominant property is hydrophobicity, these halogen atoms are not at ideal hydrophobic contact distance. Similarly, the aromatic rings of **5h** and **5i** can simultaneously be weak hydrogen bond acceptors and strongly hydrophobic, but these analogues are inappropriately shaped to make all necessary hydrophobic contacts in the pocket (see Fig. 4). Compounds **5g**, **5n–5p** have a number of structural or conformational issues as they are docked in subpocket A: there is insufficient room for the trimethoxyphenyl of **5g** or the ethoxyl-2-naphthyl of **5n**; and although the two ether oxygens of **5o** and **5p** can participate in hydrogen bonding with Cys241 β as in **2**, the methylene and ethylene, respectively, are forced to be close to the thiol sulfur and thus produce unfavorable hydrophobic–polar interactions. In contrast, the methyls of **2** can jackknife away from the sulfur.

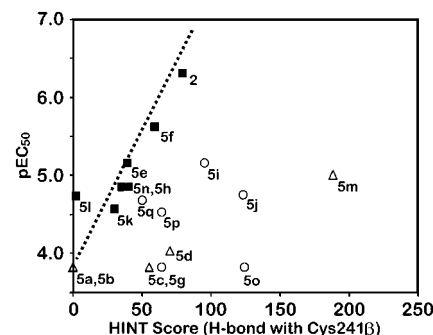


Fig. 5 HINT H-bond component score for ring interactions with Cys241 β . Closed squares represent compounds possessing both H-bond acceptors and appropriately placed hydrophobic groups. These compounds generally possess superior pEC₅₀s. Open triangles represent compounds with weak or no acceptors. Open circles represent compounds with steric issues and/or lacking key hydrophobic interactions.

two-fold; first, the hydrogen bonding interaction with Cys241 β is the key predictor, absent of steric clashes, for the microtubule inhibitory activity for this set of analogues; second, other interactions in the pocket, *i.e.*, hydrophobic, are also necessary, but competitive with this weakly scored hydrogen bonding.

The importance of both hydrophobic interactions and hydrogen bonding in subpocket A was seen in the SAR analysis and modeling studies. The latter dictates whether the C-4 analogues of pyrrole-based antitubulin agents display microtubule depolymerizing activity and the strength of that activity, while the character of the pocket requires predominantly hydrophobic moieties. Underestimation of the Cys241 β interaction was one probable reason that the total HINT score was a poor predictor of microtubule depolymerizing activity. This thiol group acts as a hydrogen bond donor and while this type of hydrogen bonding interaction is generally regarded as weak and is thusly parameterized by HINT, it is not even considered by many other scoring functions. For the downstream biological effect, microtubule depolymerization, the interaction assumed to be weak surprisingly stands out as a key factor. In fact, its absence might produce a different mechanism of action even when other portions of the structure are exactly the same, as shown particularly by **5d** with potent antiproliferative activity (0.312 μ M) but weaker microtubule depolymerization activity (\sim 94 μ M). Cys241 β has been previously identified as an important target residue for colchicine site agents.¹⁶ In a study of 15 structurally diverse colchicine site inhibitors, the docked binding modes of all included hydrogen bonding to Cys241 β (Cys239 β in that study).¹⁷ Our combined SAR and modeling study confirms the importance of that cysteine. It should be noted that there is potentially a systematic error in our procedure. As GOLD optimizes ligand placement with a different forcefield (set of rules) than used by HINT in scoring, subtle structural effects, or in this case, the interplay of several of them, are not well scored post-docking as none of the models generated by GOLD capture the set of features in a single model that HINT would score highest. This is likely to be a general observation in docking/rescoring studies, irrespective of utilized scoring functions, when subtle effects are at play.

Conclusions

We reported the synthesis, biological testing and modeling studies of C-4 analogues of pyrrole-based antitubulin agents targeting the colchicine site. For compounds that depolymerized microtubules, a linear correlation was observed between the antiproliferative activity and microtubule inhibitory activity, molecular modeling results explained the SAR very well and they both revealed that a weak hydrogen bond involved with Cys β 241 was the key determiner of microtubule depolymerizing activity, but the ideal ligand must incorporate (and properly position) this acceptor within an otherwise hydrophobic framework. Surprisingly, just the loss of that particular hydrogen bonding interaction appears to shift the antiproliferative mechanism of action away from microtubule inhibition.

This study has fairly exhaustively probed subpocket A; the 3,4-dimethoxyphenyl substituent at the pyrrole C-4 is – to date – the most ideal. The development of analogues focusing on other positions on the pyrrole core is in progress.

Acknowledgements

The excellent technical assistance of Ms Lyda Robb, Ms Cara Westbrook and Mr Nicholas Dbydal-Hargreaves is gratefully acknowledged. This work was partially supported by NIH R01 CA135043 (to D.A. Gewirtz, VCU), NIH R15 CA067236 (to JTG) and the President's Council Research Excellence Award (to SLM).

Notes and references

- 1 C. Dumontet and M. A. Jordan, *Nat. Rev. Drug Discovery*, 2010, **9**, 790.
- 2 R. A. Stanton, K. M. Gernert, J. H. Nettles and R. Aneja, *Med. Res. Rev.*, 2011, **31**, 443.
- 3 J. Griggs, J. C. Metcalfe and R. Hesketh, *Lancet Oncol.*, 2001, **2**, 82.
- 4 C. Stengel, S. P. Newman, M. P. Leese, B. V. Potter, M. J. Reed and A. Purohit, *Br. J. Cancer*, 2010, **102**, 316.
- 5 A. Tripathi, M. Fornabaio, G. E. Kellogg, J. T. Gupton, D. A. Gewirtz, W. A. Yeudall, N. E. Vega and S. L. Mooberry, *Bioorg. Med. Chem.*, 2008, **16**, 2235.
- 6 C. Da, N. Telang, P. Barelli, X. Jia, J. T. Gupton, S. L. Mooberry and G. E. Kellogg, *ACS Med. Chem. Lett.*, 2012, **3**, 53.
- 7 S. L. Mooberry, K. N. Weiderhold, S. Dakshanamurthy, E. Hamel, E. J. Banner, A. Kharlamova, J. Hempel, J. T. Gupton and M. L. Brown, *Mol. Pharmacol.*, 2007, **72**, 132.
- 8 N. Dalyot-Herman, F. Delgado-Lopez, D. A. Gewirtz, J. T. Gupton and E. L. Schwartz, *Biochem. Pharmacol.*, 2009, **78**, 1167.
- 9 J. Gupton, B. Burnham, K. Krumpe, K. Du, J. Sikorski, A. Warren, C. Barnes and I. Hall, *Arch. Pharm.*, 2000, **333**, 3.
- 10 R. B. Ravelli, B. Gigant, P. A. Curmi, I. Jourdain, S. Lachkar, A. Sobel and M. Knossow, *Nature*, 2004, **428**, 198.
- 11 A. Dorleans, B. Gigant, R. B. Ravelli, P. Mailliet, V. Mikol and M. Knossow, *Proc. Natl. Acad. Sci. U. S. A.*, 2009, **106**, 13775.
- 12 G. Jones, P. Willett and R. Glen, *J. Mol. Biol.*, 1995, **245**, 43.
- 13 SYBYL 8.1, Tripos Interactional, 1699 South Hanley Rd., St. Louis, Missouri, 63144, USA.
- 14 G. E. Kellogg and D. J. Abraham, *Eur. J. Med. Chem.*, 2000, **35**, 651.
- 15 F. Spyraakis, A. Amadasi, M. Fornabaio, D. J. Abraham, A. Mozzarelli, G. E. Kellogg and P. Cozzini, *Eur. J. Med. Chem.*, 2007, **42**, 921.
- 16 J. Chen, T. Liu, X. Dong and Y. Hu, *Mini-Rev. Med. Chem.*, 2009, **9**, 1174.
- 17 T. L. Nguyen, C. McGrath, A. R. Hermone, J. C. Burnett, D. W. Zaharevitz, B. W. Day, P. Wipf, E. Hamel and R. Gussio, *J. Med. Chem.*, 2005, **48**, 6107.